



Cite this: *J. Anal. At. Spectrom.*, 2026, 41, 308

## Cost-effective oxygen flask combustion and electrothermal vaporization capacitively coupled plasma microtorch optical emission spectrometry as a green and white method for multielemental determination in food

Augustin Catalin Mot, <sup>a</sup> Adrian-loan Dudu, <sup>ab</sup> Tiberiu Frentiu, <sup>ac</sup> Dorin Petreus, <sup>d</sup> Erika-Andrea Levei, <sup>e</sup> Zamfira Stupar, <sup>e</sup> Maria Frentiu <sup>e</sup> and Eniko Covaci <sup>\*ac</sup>

The study presents the analytical characterization of a cost-effective green and white method for the simultaneous determination of Cd, Pb, Zn, Cu, Hg, Se, and As in food using sample dissolution assisted by oxygen flask combustion and simultaneous detection by small-sized electrothermal vaporization capacitively coupled plasma microtorch optical emission spectrometry (OFC-SSETV- $\mu$ CCP-OES). Attractiveness, effectiveness and cost-efficiency of the novel method were demonstrated through the greenness and whiteness degrees evaluated using the AGREEprep software and RGB 12 algorithm, compared to traditional high-pressure microwave-assisted wet digestion and determination by inductively coupled plasma optical emission spectrometry (HP-MAWD-ICP-OES), graphite furnace atomic absorption spectrometry and thermal desorption atomic absorption spectrometry methods. Signal integration over 5 pixels along the spectral line profile provided an improvement of 2–3 fold of the limits of detection in the range of 0.01 mg kg<sup>-1</sup> (Hg, Cd, Zn) to 1.20 mg kg<sup>-1</sup> (Se), compared to the measured signal corresponding to the pixel of the emission line maximum. Validation by analysis of certified reference materials proved that the method is not affected by the non-spectral matrix effects, with recoveries and extended uncertainties in the range of 90–113% and 9–25% ( $k = 2$ ), respectively. Tukey's statistical test ( $p < 0.05$  statistical significance) and  $z$  scores revealed no bias between the results obtained by (OFC)-SSETV- $\mu$ CCP-OES, with both external calibration and the standard addition method, and those obtained by (HP-MAWD)-ICP-OES with external calibration. The applicability of the method was demonstrated through the analysis of fish tissue, mushroom, and dietary supplement samples, with precision ranging from 4.9% to 14.5%. The (OFC)-SSETV- $\mu$ CCP-OES method presented a greenness score of 77%, evaluated by the AGREEprep metric, while the redness, greenness, blueness and whiteness scores, evaluated by the RGB 12 algorithm, were 86%, 94%, 98% and 93%. The scores are related to the combination of representative features of sample preparation by OFC, namely virtually energy-free processing, reduced reagents consumption and generated waste, along with the potential of simple and cost-effective miniaturized instrumentation for the simultaneous determination of trace elements in a low power (15 W) and low Ar consumption (150 mL min<sup>-1</sup>) microplasma source, which are essential for greater chemical sustainability in analytical procedures compared to conventional methods.

Received 2nd August 2025  
Accepted 27th October 2025

DOI: 10.1039/d5ja00297d

rsc.li/jaas

<sup>a</sup>Babeş-Bolyai University, Faculty of Chemistry and Chemical Engineering, Arany Janos 11, 400028 Cluj-Napoca, Romania. E-mail: eniko.covaci@ubbcluj.ro

<sup>b</sup>Enzymology and Applied Biocatalysis Research Center, Faculty of Chemistry and Chemical Engineering, Babeş-Bolyai University, Arany Janos 11, 400028 Cluj-Napoca, Romania

<sup>c</sup>Babeş-Bolyai University, Research Center for Advanced Analysis, Instrumentation and Chemometrics, Arany Janos 11, 400028 Cluj-Napoca, Romania

<sup>d</sup>Technical University of Cluj-Napoca, Faculty of Electronics, Telecommunications and Information Technology, Gheorghe Baritiu 26-28, 400027 Cluj-Napoca, Romania

<sup>e</sup>National Institute for Research and Development of Optoelectronics INOE 2000, Research Institute for Analytical Instrumentation Subsidiary, Donath 67, 400293 Cluj-Napoca, Romania

## Introduction

Sample preparation techniques for elemental analysis, selected according to the type of matrix and the analytes, should ensure their conversion into a form readily accessible to the employed spectrometric method, in order to achieve the best analytical performance.<sup>1–3</sup> In the case of solid samples, the development of quicker and easier preparation strategies, such as direct sampling from the solid matrix, as well as various time- and energy-efficient extraction procedures that maintain comparable effectiveness to traditional methods based on organic



matrix destruction coupled with quantification using more sensitive detectors in miniaturized instrumentation, has emerged as alternatives to traditional approaches generally based on high-pressure microwave-assisted wet digestion (HP-MAWD) using concentrated acids.<sup>4,5</sup> However, alternative dissolution methods, such as microwave-induced combustion and oxygen flask combustion (OFC), have been employed together with multielemental spectrometric techniques based on inductively coupled plasma optical emission spectrometry (ICP-OES), inductively coupled plasma mass spectrometry, atomic absorption spectrometry, and atomic fluorescence spectrometry for the determination of trace metals and nonmetals with or without chemical vapor generation in organic matrices, such as biological samples, foodstuffs of vegetable and animal origin, graphitic and organic polymeric materials, fuels, and even environmental samples with high carbon content.<sup>6-20</sup> Microwave induced combustion and OFC procedures offer significant advantages for sample preparation, such as: (i) the use of small amounts of additional reagents alongside oxygen for combustion; (ii) low volumes and concentrations of reagents used for the absorption and dissolution of analytes released during combustion, typically between 0.1 and 1 mol L<sup>-1</sup> HNO<sub>3</sub>, HCl, NH<sub>4</sub>OH, etc.; (iii) low waste generation; (iv) reduced energy consumption and a fast combustion process; and (v) simple sample handling. Such approaches could be a support in the development of multi-elemental analytical techniques with high greenness, redness, blueness, and whiteness performance metrics, by coupling with cost-effective instrumentation based on a microplasma source and a low-resolution microspectrometer for the determination of both priority hazardous elements and essential trace elements in food. To the best of our knowledge, such an approach has not yet been reported in the literature.

A comprehensive evaluation of the analytical method colours, which includes not only the greenness related to sample preparation, but also the redness reflecting figures of merit or analytical performance, and the blueness encompassing indicators of practical applicability, cost-effectiveness and functional features, is a crucial approach in modern analytical chemistry. The evaluation of the whiteness degree of a new analytical method represents a balance between the colours of the method, depending on the specific characteristics of the method, as certain criteria associated with one colour may be more prominent than others. Nonetheless, all contribute to the overall whiteness score, expressed on a scale up to 100%, which reflects whether the evaluated method is fit-for-purpose across a broad spectrum of parameters included in the proposed model.<sup>21-29</sup>

We have demonstrated that coupling diffusive gradients in thin films passive sampling, performed *in situ* for surface waters and *ex situ* for soil samples, with small-sized electrothermal vaporization capacitively coupled plasma microtorch optical emission spectrometry (SSETV- $\mu$ CCP-OES), not only improves the detection limits of the elements' labile fractions in water and soil, but also enables the development of simultaneous multielement methods characterized by a high degree of greenness and whiteness. These advantages are especially

significant when compared to traditional techniques commonly used in environmental monitoring laboratories, such as graphite furnace atomic absorption spectrometry (GFAAS) and thermal desorption atomic absorption spectrometry (TDAAS).<sup>30,31</sup>

The aim of this study was to develop and validate a cost-effective method by coupling the OFC sample preparation procedure with simultaneous multielemental detection using SSETV- $\mu$ CCP-OES for the determination of several elements relevant to food monitoring and human health, such as Cd, Pb, Zn, Cu, Hg, Se and As. The (OFC)-SSETV- $\mu$ CCP-OES method was validated based on limits of detection (LODs), accuracy, and precision, assessed through the analysis of certified reference materials (CRMs) and comparison with traditional techniques, namely the single element determination of Hg by TDAAS, the sequential GFAAS, and the simultaneous determination by ICP-OES, the latter applied with chemical vapor generation for As, Hg, and Se under previously established prereduction and derivatization conditions.<sup>32</sup> The influence of the pixel number for signal integration across the episodic spectral line profile was evaluated in terms of method sensitivity, calibration curve linearity, and LODs, in comparison with signal integration based on a single pixel corresponding to the spectral line maximum. The optimal number of pixels for signal integration along the line profile yielding the best LODs, evaluated according to the signal-to-background ratio and relative standard deviation of the background (SBR-RSDB) procedure, was established.<sup>33,34</sup> The advantages of the new (OFC)-SSETV- $\mu$ CCP-OES method in terms of analytical performance, utility, and applicability were highlighted through its greenness, evaluated by the AGREEprep metric, and its whiteness, assessed *via* the RGB 12 algorithm.<sup>21,22</sup>

## Materials and methods

### Instrumentation

A schematic representation of the (OFC)-SSETV- $\mu$ CCP-OES experimental setup is shown in Fig. 1. The functional details of the SSETV- $\mu$ CCP-OES experimental setup have been

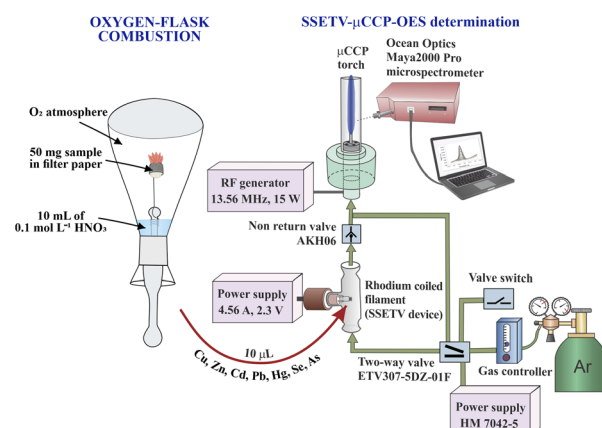


Fig. 1 Schematic representation of the (OFC)-SSETV- $\mu$ CCP-OES experimental setup.



previously described.<sup>30</sup> The system consists of a capacitively coupled plasma microtorch (Babeş-Bolyai University, Cluj-Napoca, Romania) operated at 15 W and 150 mL min<sup>-1</sup> Ar, powered by a miniaturized 13.56 MHz radiofrequency generator (Technical University of Cluj-Napoca, Romania), interfaced with a Maya2000 Pro microspectrometer (Ocean Optics, Dunedin, USA) purged with high-purity N<sub>2</sub> 6.0 covering a spectral range of 165–309 nm with a full width at half maximum of 0.35 nm.<sup>35,36</sup> The vapour generated *via* the miniaturized SSETV device (Babeş-Bolyai University, Cluj-Napoca, Romania) from a 10 µL liquid microsample was introduced into the microplasma source by electrothermal evaporation from a Rh microfilament with 250 µm diameter and 99.9% purity (Goodfellow, Cambridge, UK).<sup>35</sup> The microfilament was heated using the TENMA 72-13360 programmable power supply (TENMA Inc., China) at 80 °C (0.25 V and 1.93 A) for 180 s for sample drying and at 1500 °C (2.3 V and 4.56 A) for 10 s for sample vaporization. These conditions enabled multielement evaporation and simultaneous recording of 3D episode emission spectra (signal-wavelength-time) with an integration time of 100 ms per episodic spectrum. Radial spectroscopic observation of the microplasma was performed through a collimating lens with 10 mm focal length without fibre optics, at a height of 0.8 mm above the Mo microelectrode tip. The observation height was adjusted with an increment of 100 µm using a 3D translator on which the microspectrometer was mounted. Thermal calibration of the Rh microfilament was carried out over two temperature ranges of 50–600 °C and 800–1600 °C by measuring the filament temperature using the 3ML-CF1 and 1MH1-CF3 IR sensors (Optris GmbH & Co.KG, Berlin, Germany).<sup>37</sup> The TENMA 72-13360 power supply enabled a temperature control of the microfilament with a precision better than ±15 °C and an accuracy of at least ±20 °C, at a target value of 1500 °C for 7 s after the filament reached the set temperature in approximately 3 seconds from the start of heating.<sup>30</sup> A SMCEVT307-5 DZ-01 F-Q two-way valve powered by the HY3003 Mastech supply (Premier Farnell, Leeds, UK) was inserted into the argon flow path to control its route during the drying and vaporization stage. These operating conditions ensured highly reproducible evaporation of the microsample, as well as recording of episodic emission spectra for all elements.

A Spectro CIROS<sup>CCD</sup> simultaneous ICP-OES spectrometer (Spectro, Kleve, Germany) was used for Cu, Zn, Cd and Pb determination in samples prepared by HP-MAWD under measurement conditions previously described.<sup>37</sup> For the determination of Hg, As and Se by chemical vapor generation, a HGX-200 hydride/cold vapor generator (Teledyne CETAC Technologies, Omaha, Nebraska, USA) was coupled to the ICP spectrometer.<sup>32</sup>

A Berghof MW3 S+ digester (Berghof, Germany) was employed for sample preparation, according to the previously reported HP-MAWD procedure.<sup>32</sup>

Total carbon (TC), total organic carbon (TOC) and total inorganic carbon (TIC) fractions were quantified using a Multi N/C 2100S Analyzer (Analytik Jena, Jena, Germany) in accordance with ISO 20236:2024.<sup>38</sup>

## Reagents, standard solutions, certified reference materials and food samples

All reagents and standard solutions used in this study for sample preparation were purchased from Merck (Darmstadt, Germany). Single-element standard solutions of Cd, Cu, Pb, Zn, Hg, As and Se (1000 mg L<sup>-1</sup>) were used to prepare the multielement calibration standards in 2% (v/v) HNO<sub>3</sub> over the concentration range of 0.01–0.10 mg L<sup>-1</sup> Cd, Hg and Zn, 0.10–1.00 mg L<sup>-1</sup> Cu and Pb, and 0.10–2.00 mg L<sup>-1</sup> As and Se. Certified reference materials, namely Tort-3 lobster hepatopancreas (National Research Council Canada, Ottawa, Ontario, Canada), CE278k mussel tissue (Institute for Reference Materials and Measurements – IRMM, Geel, Belgium), CS-M-3 dried mushroom powder (*Boletus edulis*) (Institute of Nuclear Chemistry and Technology, Warsaw, Poland), GBW 10011 wheat (Institute of Geophysical and Geochemical Exploration, Langfang, China) and SRM 3280 multivitamin/multielement tablets (National Institute of Standards and Technology, Gaithersburg, USA) were used to check the accuracy (recovery and precision) of the (OFC)-SSETV-µCCP-OES method. Ultrapure water was produced in the laboratory using a Milli-Q system (Millipore, Bedford, USA). Solution of 0.1 mol L<sup>-1</sup> HNO<sub>3</sub> was used as absorbing medium and sample dissolution by combustion. A solution of 0.1 mol L<sup>-1</sup> HCl was used for the decomposition of TIC in solid samples. All glassware was decontaminated by soaking for 12 hours in 10% (v/v) HNO<sub>3</sub> and subsequently rinsed with ultrapure water. The combustion flask and the platinum sample holder were sequentially washed between combustions with 10% (v/v) HNO<sub>3</sub>, ultrapure water and acetone, whereas after each working day the platinum basket was kept overnight in concentrated HNO<sub>3</sub> for decontamination. Fish samples and dietary supplements were purchased from supermarkets and pharmacies in Cluj-Napoca, Romania, while mushroom samples were collected from forests in the surrounding area.

## Sample preparation by OFC-assisted dissolution

The combustion of samples was carried out using a 500 mL or 1000 mL quartz Schöniger-type Erlenmeyer flask manufactured by Exeter Analytical (Coventry, UK), equipped with a platinum basket (20 × 7 mm), manufactured by Elemental Microanalysis Ltd (Okehampton, Devon, UK) (Fig. 1). Amounts of 50 mg homogenized powdered CRMs and food samples were weighed directly onto 3 cm × 2 cm pieces of Whatman® Grade 542 hardened ashless quantitative filter paper, wrapped and placed in the platinum basket attached to the Erlenmeyer flask stopper. A volume of 10 mL of 0.1 mol L<sup>-1</sup> HNO<sub>3</sub> absorbent solution was introduced into the flask to retain the gases generated during combustion. The flask was then purged with 5.0 grade oxygen for 5 minutes at a flow rate of 1 L min<sup>-1</sup>. The filter paper containing the sample was manually ignited and immediately inserted into the Erlenmeyer flask through the stopper and hermetically sealed. Combustion was carried out with the flask positioned upside down to prevent gas losses. The resulting gases were absorbed over a 10-minute period into the nitric acid solution by manually stirring the flask every 2



minutes. Multielement determinations were performed directly in the absorbent solution after centrifugation at 3000 rpm for 10 min. A blank sample was prepared by combusting a sample-free filter paper. The sample amount of 50 mg and the 500 mL or 1000 mL combustion flask were selected based on the combustion capacity of the system, which depends on the amount of oxygen required for efficient combustion of carbon-rich matrices such as food samples.<sup>7</sup>

### (OFC)-SSETV- $\mu$ CCP-OES method validation

The (OFC)-SSETV- $\mu$ CCP-OES method was validated based on LODs, accuracy, and precision. Instrumental LODs were evaluated based on the SBR-RSDB approach ( $LOD = 3 \times 0.01 \times RSDB \times c/SBR$ ).<sup>33,34</sup> The RSDB is the relative standard deviation of the background (%) calculated from the background signal of 11 episodic spectra recorded before the appearance of the analyte signal, considering 1, 3, 5 and 7 pixels similar to the number of pixels used in the integration of the analyte signal over the spectral line profile. The SBR is the signal-to-background ratio for an analyte concentration within the calibration range. The analyte signals used in the calibration curve plotting were obtained by 3D integration (signal-wavelength-time), according to the number of pixels used to integrate the signal over the spectral line profile ( $CP \pm n$ ) from each episodic spectrum. CP corresponds to the pixel of the emission line maximum, while  $n = 1, 2, 3$  correspond to the pixels on the wings of the line profile relative to CP. The dependence of the calibration curve slope, RSDB, SBR and LODs *versus* the number of integrating pixels of the signal was evaluated, and the number of pixels that yielded the best LODs was selected. The LODs obtained by (OFC)-SSETV- $\mu$ CCP-OES were compared with values obtained in our laboratory using traditional spectrometric methods, such as GFAAS, ICP-OES with chemical vapor generation for Hg, As, and Se, and TDAAS for Hg. The linearity of the calibration curves was checked using Mandel's test.<sup>39</sup>

Analyte recovery in the CRM samples was evaluated against the certified concentration and the expanded uncertainty at a coverage factor of  $k = 2$ , corresponding to a 95% confidence level. Additionally, the  $z$ -score was calculated according to the European Guidelines for the validation of analytical methods.<sup>40</sup> The magnitude of non-spectral matrix interferences in the (OFC)-SSETV- $\mu$ CCP-OES method, which may cause bias from the target value, was assessed by comparing the results obtained for CRMs using external calibration and the standard addition method. The results obtained in CRM samples by the (OFC)-SSETV- $\mu$ CCP-OES method were also validated by comparison with HP-MAWD in a  $HNO_3$ - $H_2O_2$  mixture and determination by ICP-OES. Tukey's statistical test<sup>41</sup> ( $p < 0.05$  statistical significance) was used to check any possible bias between the results obtained with (OFC)-SSETV- $\mu$ CCP-OES and (HP-MAWD)-ICP-OES. A study of the combustion efficiency (%) of the samples, according to the volume of the employed flask, was carried out. Combustion efficiency was evaluated based on the TOC weight in the solid sample, the absorbing solution, and any potential unburned carbon residue. Total carbon in solid was measured directly by combustion at 1100 °C, while TOC was determined

after removal of TIC by treating the solid sample with 0.1 mL of 1 mol L<sup>-1</sup> HCl for 30 min directly in the sample boat. In liquid samples potentially containing particles in suspension, the determinations were performed by catalytic oxidation at 800 °C. Sample homogeneity was ensured by initial vortexing for 2 min, followed by continuous stirring (speed level 8) during sampling.

### Greenness and whiteness evaluation by the AGREEprep metric and RGB 12 algorithm

The AGREEprep metric is based on 10 assessment steps corresponding to the green sample preparation principles.<sup>21</sup> This metric was selected because it more effectively accounts for the environmental impact of sample preparation and enables a more accurate evaluation of energy consumption and waste generation, compared to other metrics in which these aspects are poorly defined and difficult to quantify. The AGREEprep metric was carried out using the open-access software available through the link indicated in the paper.<sup>21</sup> The software generates a pictogram through which the performance of the method is intuitively visualised and allows rapid identification of the strengths and weaknesses of the method.

The RGB 12 metric includes 12 criteria, divided into four for each of the red, green, and blue components using the Excel worksheet provided as the SI to the paper.<sup>22</sup> Therefore, the RGB 12 model was used because it is an evidence-based method, sufficiently flexible, which demands the evaluator to rigorously adapt all 12 individual parameters in assessing the whiteness degree.

The performance indicators of (OFC)-SSETV- $\mu$ CCP-OES, highlighted by the colours, were compared with those of (HP-MAWD)-SSETV- $\mu$ CCP-OES and (HP-MAWD)-ICP-OES with chemical vapor generation for As, Se, and Hg, GFAAS and TDAAS for Hg, respectively. This ensured a structured evaluation and enabled a clear identification of advantages compared to the reference methods.

## Results and discussion

### Efficiency of sample combustion

The concentrations of TC, TIC and TOC in the analysed food samples and absorbing liquid potentially containing particles in suspension, for the combustion of a 50 mg sample in a 500 mL flask, are presented in the SI (Table S1). The combustion efficiency, presented in the same table, was calculated from the mass balance of the TOC fraction in the solid sample, and the residual TOC in absorbing liquid containing any remaining suspended matter. The TOC fraction in the analysed food was predominant, ranging from 45% to 99%, with lower weights corresponding to the dietary supplements. In the absorbing liquid, TOC concentrations ranged from 8.2 to 50.2  $\mu$ g mL<sup>-1</sup>, whereas TIC represented the largest fraction (39–89%), due to the absorbed CO<sub>2</sub> resulting from the combustion. This observation is consistent with the results obtained for liquid samples purged with nitrogen, in which the TIC fraction was below the LOD of the method (1  $\mu$ g mL<sup>-1</sup>), with only the dissolved organic fraction being determined.



The combustion efficiency for 50 mg of GBW 10011 (Wheat) and Tort-3 (Lobster hepatopancreas) CRMs *versus* flask volume (250, 500 and 1000 mL) is presented in the SI (Fig. S1). The combustion efficiency was  $90.1 \pm 7.3\%$  for GBW 10011 and  $96.3 \pm 7.2\%$  for Tort-3 in the case of the 250 mL flask. The incomplete combustion was evidenced by the residual material remaining in the platinum basket. Therefore, the flask volume was increased to 500 and 1000 mL, yielding an increase in the combustion efficiency to  $98.1 \pm 6.8\%$  and  $99.9 \pm 6.7\%$  for Tort-3, and  $99.6 \pm 6.2\%$  and  $99.9 \pm 7.1\%$  for GBW 10011. The same phenomenon was observed in the case of other samples, as indicated in the SI (Table S1). Increasing the flask volume to 500 mL effectively prevented incomplete combustion, with residues ranging from 0.2 to 20 mg. The higher quantities corresponded to the dietary supplements with low TOC content, which was also highlighted in the remaining residue. In the case of the 1000 mL flask, combustion was virtually complete, with no detectable residue on the platinum basket. However, a 500 mL vessel was considered sufficient for the combustion of the food samples under study.

### Element vaporization from the Rh microfilament

The operating conditions of the miniaturized SSETV and  $\mu$ CCP-OES tandem should ensure both efficient and high flow rate of the microsample vapor into the microplasma by instantaneous vaporization, so that simultaneous analysis is feasible.<sup>31</sup> Fig. 2 presents the episodic emission spectra recorded by evaporation of a 10  $\mu$ L microsample containing  $0.1 \text{ mg L}^{-1}$  Cd, Zn, and Hg;  $1 \text{ mg L}^{-1}$  Cu and  $2 \text{ mg L}^{-1}$  Se, from a Rh filament heated to  $1500 \pm 20 \text{ }^\circ\text{C}$  (2.3 V, 4.56 A) for 10 s, interfaced with microplasma

operated at 15 W,  $150 \text{ mL min}^{-1}$  Ar flow, and 0.8 mm spectroscopic observation height above the Mo tip microelectrode. The emission spectrum of arsenic was recorded separately using a single element solution of  $2 \text{ mg L}^{-1}$  as a result of spectral interference of the As 228.812 nm line with that of Cd at 228.802 nm. The operating parameters of the experimental set-up were selected based on previously reported results in the analysis of food and environmental samples prepared by the HP-MAWD procedure.<sup>37</sup>

Fig. 3 presents the transient signals of the analytes at the most sensitive spectral lines resulting from the episodic emission, recorded with an integration time of 100 ms at  $\text{CP} \pm 2$  pixels. The shape of the emission spectra, with maxima at 1.8 s (Hg), 3.6 s (Se), 4.5 s (Cd), 4.9 s (Pb), 5.0 s (As), 5.2 s (Zn) and 5.5 s (Cu), indicates a temporal evaporation behaviour dependent on the nature of the elements, during the 10 s heating time of the filament. A selective evaporation of Hg is evident, but no separation of the Cd 228.802 nm emission from that of As at 228.812 nm was achieved.

### Calibration curves, sensitivity and LODs dependence on the integrating pixels of the signal over the spectral line profile

The relationship between the calibration curves obtained by the SSETV- $\mu$ CCP-OES method for different numbers of pixels for signal integration over the spectral line profile is illustrated in the SI (Fig. S2). The same dependence for SBR, RSDB and LODs is presented in the SI (Fig. S3–S5).

According to Fig. S2, an enhancement of sensitivity of 4.2 to 4.7 times, depending on the element, was observed by increasing the number of integrating pixels to 7. The

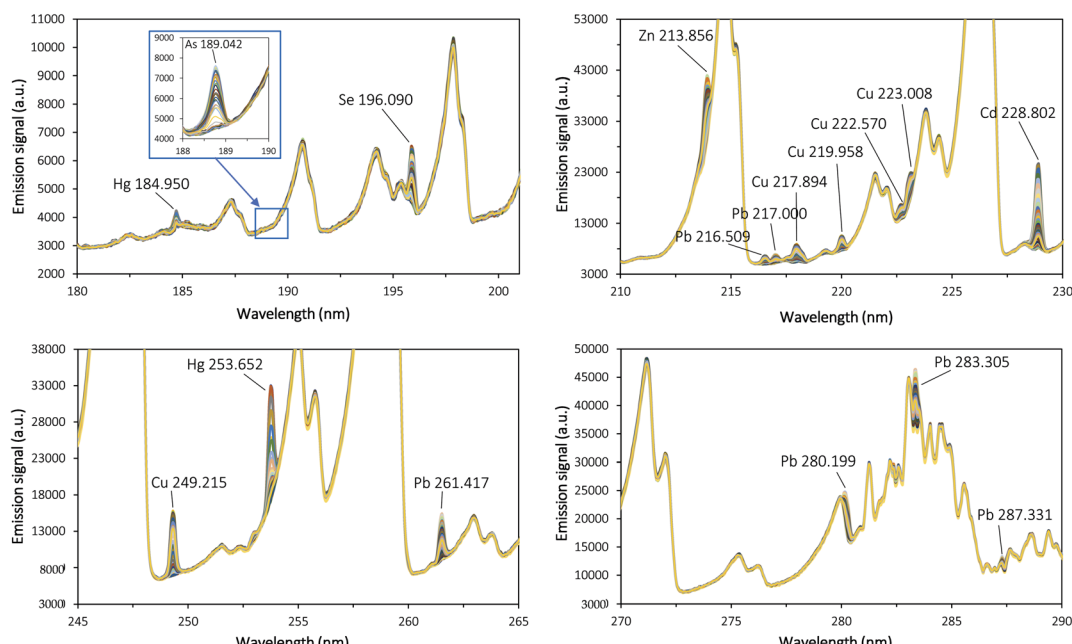


Fig. 2 Episodic emission spectra recorded by the SSETV- $\mu$ CCP-OES method for a multielement solution containing  $0.1 \text{ mg L}^{-1}$  Cd, Zn, Hg;  $1 \text{ mg L}^{-1}$  Cu and  $2 \text{ mg L}^{-1}$  Se. Arsenic was measured using a single element solution of  $2 \text{ mg L}^{-1}$ . Measurement conditions: 15 W plasma power,  $150 \text{ mL min}^{-1}$  Ar flow rate, 0.8 mm observation height above the Mo tip electrode, 100 episodic spectra recording with 100 ms integration time per episode, and Rh filament heating at  $1500 \pm 20 \text{ }^\circ\text{C}$  for 10 s.



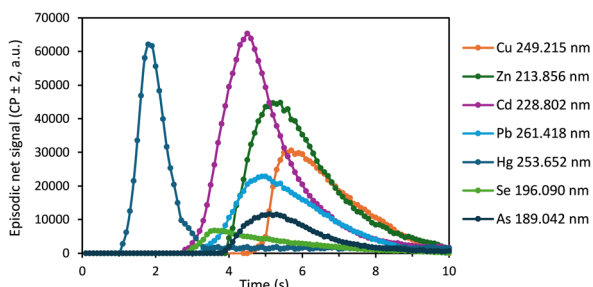


Fig. 3 Transient signals ( $CP \pm 2$ ) of the elements at their most sensitive spectral lines for a  $10 \mu\text{L}$  aliquot sample containing  $0.1 \text{ mg L}^{-1}$  Cd, Zn, Hg,  $1 \text{ mg L}^{-1}$  Cu and  $2 \text{ mg L}^{-1}$  Se. Arsenic was measured using a single element solution of  $2 \text{ mg L}^{-1}$ . Measurement conditions:  $80^\circ\text{C}$  for  $180 \text{ s}$  sample drying,  $1500 \pm 20^\circ\text{C}$  for  $10 \text{ s}$  sample vaporization,  $15 \text{ W}$  plasma power,  $150 \text{ mL min}^{-1}$  Ar flow rate,  $0.8 \text{ mm}$  observation height above the Mo tip microelectrode,  $100$  episodic spectra recorded with  $100 \text{ ms}$  integration time per episode.

determination coefficients ( $R^2$ ) of the calibration curves were in the range of  $0.9987$  to  $0.9994$  for signal integration over  $1$  to  $7$  pixels along the spectral line profile. However, the Mandel statistical test confirmed linearity over the studied calibration ranges, regardless of the pixel number, with experimental  $F_{\text{exp}}$  values of up to  $4.42$ , which were lower than the tabulated  $F_{\text{tab},(95\%,1,n-3)} = 10.13$ . A dependence according to a second-degree equation for the SBR was obtained, and consequently, an increase of  $3.7$  to  $4$  times for a number of  $5$  pixels compared to the SBR resulted at the CP (SI, Fig. S3) was obtained. The RSDB ranged between  $0.5\%$  and  $6.0\%$ , showing an increase with the number of pixels considered for background signal averaging (SI, Fig. S4). The increase is attributed to the variation of the background signal with wavelength, due to the line position of As  $189.042 \text{ nm}$  and Se  $196.090 \text{ nm}$  on the line-wings of molecular  $\text{O}_2$  emission ( $175$ – $205 \text{ nm}$ ,  $B^3\Sigma_u^- - X^3\Sigma_g^-$ , Schuman–Runge transition), and Zn  $213.856 \text{ nm}$  and Hg  $253.652 \text{ nm}$  on the line wings of molecular NO emission ( $200$ – $300 \text{ nm}$ ,  $X^2\Pi \rightarrow A^2\Sigma^+$  transition). Considering the dependence of SBR and RSDB *versus* the number of pixels, the best LODs were achieved when integrating the signal over  $5$  pixels along the spectral line profile

Table 1 LODs for the (OFC)-SSETV- $\mu$ CCP-OES method obtained by the SBR-RSDB approach with signal integration over  $5$  pixels of the analytical line compared with ICP-OES, GFAAS and TDAAS methods

Element	SSETV- $\mu$ CCP-OES			GFAAS		
	$\mu\text{g L}^{-1}$	$\text{mg kg}^{-1}$	pg	ICP-OES ( $\text{mg kg}^{-1}$ )	$\text{mg kg}^{-1}$	pg
Hg	0.05	0.010	0.5	0.04 <sup>a</sup>	0.004 <sup>b</sup>	0.0008
Cu	0.14	0.030	1.4	0.62	0.030	3.0
Zn	0.04	0.010	0.4	0.04	0.020	1.6
Pb	0.35	0.070	3.5	0.85	0.030 <sup>c</sup>	3.0
Cd	0.05	0.010	0.5	0.06	0.006 <sup>c</sup>	0.6
Se	6.0	1.20	60	0.05 <sup>a</sup>	—	—
As	5.0	1.00	50	0.06 <sup>a</sup>	0.020 <sup>c</sup>	2.0

<sup>a</sup> Obtained by CV(HG)-ICP-OES. <sup>b</sup> Obtained by TDAAS. <sup>c</sup> Chemical modifiers: As:  $0.1\%$   $\text{Pd}(\text{NO}_3)_2 + 0.06\%$   $\text{Mg}(\text{NO}_3)_2$ ; Pb and Cd:  $1\%$   $\text{NH}_4\text{H}_2\text{PO}_4 + 0.06\%$   $\text{Mg}(\text{NO}_3)_2$ .

(SI Fig. S5). The instrumental LODs obtained by the SBR-RSDB approach for the SSETV- $\mu$ CCP-OES method with analytical signal integration over  $5$  pixels, together with those obtained in the analysis of food samples subjected to OFC, are presented in Table 1. The LODs obtained by ICP-OES with pneumatic nebulization and chemical vapor generation for As, Se and Hg, and those obtained by GFAAS and TDAAS, are illustrated for comparison.

The instrumental LODs of the SSETV- $\mu$ CCP-OES method for  $5$  pixels were in the range  $0.04 \text{ }\mu\text{g L}^{-1}$  (Zn) to  $6.0 \text{ }\mu\text{g L}^{-1}$  (Se). The analytical signal integration over  $5$  pixels along the spectral line profile resulted in an improvement of LODs generally  $2$ – $3$  times compared to those obtained in the case of the CP signal corresponding to the emission line maximum. In the case of Zn, the improvement was only  $1.25$ -fold due to the significant increase in RSDB values, rising from  $0.8\%$  for a single pixel to  $2.4\%$  and  $3.2\%$  for  $5$  and  $7$  pixels, respectively, despite achieving an SBR enhancement of  $3.7$  and  $4.2$  times. The significant increase of RSDB in the case of Zn  $213.856 \text{ nm}$  is due to the position of the analytical line on the line-wing of  $214.91 \text{ nm}$  associated with the NO molecular emission band ( $5.45 \text{ eV}$ ,  $X^2\Pi \rightarrow A^2\Sigma^+$  transition), which causes a significant variation of the background signal, as shown previously. The (OFC)-SSETV- $\mu$ CCP-OES method provides LODs of  $0.01 \text{ mg kg}^{-1}$  (Hg, Cd, Zn);  $0.030 \text{ mg kg}^{-1}$  (Cu);  $0.070 \text{ mg kg}^{-1}$  (Pb);  $1.00 \text{ mg kg}^{-1}$  (As) and  $1.20 \text{ mg kg}^{-1}$  (Se) in foodstuffs, for  $50 \text{ mg}$  samples subjected to OFC and dissolution in  $10 \text{ mL}$   $0.1 \text{ mol L}^{-1}$   $\text{HNO}_3$ . The LODs are better for Zn, Cd, Cu, and Pb compared to sample preparation by HP-MAWD and ICP-OES measurement with pneumatic nebulization, and similar to the LOD for Hg achieved by CV-ICP-OES. The LODs obtained for Se and As by the (OFC)-SSETV- $\mu$ CCP-OES method without chemical vapor generation are significantly poorer compared to HG-ICP-OES ( $0.05$  and  $0.06 \text{ mg kg}^{-1}$ ). A LOD of  $1.4 \text{ }\mu\text{g L}^{-1}$  and  $0.5 \text{ mg kg}^{-1}$  for As was previously achieved by the HG- $\mu$ CCP-OES method.<sup>42</sup> The LODs are similar for Cu, and apparently, about two times better for Zn, and two times poorer for Pb and Cd compared to GFAAS. However, it is important to consider the microsample volume of  $10 \mu\text{L}$  for SSETV- $\mu$ CCP-OES *versus*  $20 \mu\text{L}$  in GFAAS. Therefore, the absolute LODs (pg) in the (OFC)-SSETV- $\mu$ CCP-OES method were in the range of  $0.4$  (Zn) to  $3.5$  (Pb), comparable with those obtained by GFAAS. The LOD was much poorer for As compared to GFAAS, but differences in instrumental components, which largely determine method sensitivity, should also be considered. The LOD for Hg in the SSETV- $\mu$ CCP-OES method is four times poorer compared to TDAAS, but the sample amount should also be considered, namely  $200 \text{ mg}$  for TDAAS *versus*  $50 \text{ mg}$  dissolved in  $10 \text{ mL}$  absorption solution for the SSETV- $\mu$ CCP-OES method.

#### Accuracy of the (OFC)-SSETV- $\mu$ CCP-OES method

Table 2 presents the results for the CRMs (mean and expanded uncertainty,  $k = 2$ ) obtained by SSETV- $\mu$ CCP-OES using both external calibration and the standard addition method, compared to the certified values.

According to Table 2, there is good agreement between the found values obtained from both the external calibration and



Table 2 Found concentrations for Cu, Zn, Cd, Pb, Hg, Se and As in vegetables and meat-based CRMs obtained by the (OFC)-SSETV- $\mu$ CCP-OES method

CRM	Calibration (mg kg <sup>-1</sup> )	Cu			Zn			Cd			Pb			Hg			Se			As		
		Certified value $\pm$ $U_{CRM}^a$	Found value $\pm$ $U_{lab}^b$	Certified value $\pm$ $U_{CRM}^a$	Found value $\pm$ $U_{lab}^b$	Certified value $\pm$ $U_{CRM}^a$	Found value $\pm$ $U_{lab}^b$	Certified value $\pm$ $U_{CRM}^a$	Found value $\pm$ $U_{lab}^b$	Certified value $\pm$ $U_{CRM}^a$	Found value $\pm$ $U_{lab}^b$	Certified value $\pm$ $U_{CRM}^a$	Found value $\pm$ $U_{lab}^b$	Certified value $\pm$ $U_{CRM}^a$	Found value $\pm$ $U_{lab}^b$	Certified value $\pm$ $U_{CRM}^a$	Found value $\pm$ $U_{lab}^b$	Certified value $\pm$ $U_{CRM}^a$	Found value $\pm$ $U_{lab}^b$	Certified value $\pm$ $U_{CRM}^a$	Found value $\pm$ $U_{lab}^b$	
		(mg kg <sup>-1</sup> )	(mg kg <sup>-1</sup> )	(mg kg <sup>-1</sup> )	(mg kg <sup>-1</sup> )	(mg kg <sup>-1</sup> )	(mg kg <sup>-1</sup> )	(mg kg <sup>-1</sup> )	(mg kg <sup>-1</sup> )	(mg kg <sup>-1</sup> )	(mg kg <sup>-1</sup> )	(mg kg <sup>-1</sup> )	(mg kg <sup>-1</sup> )	(mg kg <sup>-1</sup> )	(mg kg <sup>-1</sup> )	(mg kg <sup>-1</sup> )	(mg kg <sup>-1</sup> )	(mg kg <sup>-1</sup> )	(mg kg <sup>-1</sup> )	(mg kg <sup>-1</sup> )	(mg kg <sup>-1</sup> )	
Tort-3 (lobster hepatopancreas)	Ext. calib.	497 $\pm$ 22	515 $\pm$ 63	136 $\pm$ 6	146 $\pm$ 16	42.3 $\pm$ 1.8	39.6 $\pm$ 5.5	0.225 $\pm$ 0.018	0.249 $\pm$ 0.044	0.292 $\pm$ 0.022	0.328 $\pm$ 0.046	10.9 $\pm$ 1.0	11.9 $\pm$ 2.4	59.5 $\pm$ 3.8	53.7 $\pm$ 8.4							
	Std. add.	524 $\pm$ 66		147 $\pm$ 17		41.5 $\pm$ 3.8		0.238 $\pm$ 0.047		0.319 $\pm$ 0.052		12.0 $\pm$ 3.2		63.5 $\pm$ 12.1								
CE278k (mussel tissue)	Ext. calib.	5.98 $\pm$ 0.27	6.35 $\pm$ 0.98	71 $\pm$ 4	66 $\pm$ 6	0.336 $\pm$ 0.025	0.357 $\pm$ 0.064	2.18 $\pm$ 0.18	2.09 $\pm$ 0.46	0.071 $\pm$ 0.007	0.072 $\pm$ 0.018	1.62 $\pm$ 0.12	<3.96 (LOQ)	6.7 $\pm$ 0.4	6.5 $\pm$ 1.2							
	Std. add.	5.77 $\pm$ 1.36		73 $\pm$ 11		0.371 $\pm$ 0.048		2.10 $\pm$ 0.50		0.079 $\pm$ 0.020		<3.96 (LOQ)		6.9 $\pm$ 1.6								
CS-M-3 (dried mushroom powder)	Ext. calib.	18.73 $\pm$ 0.70	18.72 $\pm$ 2.81	113.30 $\pm$ 3.28	106.05 $\pm$ 16.23	1.229 $\pm$ 0.110	1.195 $\pm$ 0.291	1.863 $\pm$ 0.108	1.943 $\pm$ 0.330	2.849 $\pm$ 0.104	3.137 $\pm$ 0.445	17.43 $\pm$ 1.36	18.69 $\pm$ 3.74	0.651 $\pm$ 0.026 (LOQ)	<3.30 (LOQ)							
	Std. add.	20.83 $\pm$ 4.15		105.63 $\pm$ 18.21		1.285 $\pm$ 0.325		1.691 $\pm$ 0.343		2.796 $\pm$ 0.448		17.56 $\pm$ 4.25		<3.30 (LOQ)								
GBW 10011 (wheat)	Ext. calib.	2.7 $\pm$ 0.2	2.5 $\pm$ 0.4	11.6 $\pm$ 0.7	12.1 $\pm$ 2.3	18 $\pm$ 4	19 $\pm$ 5	0.065 $\pm$ 0.024	<0.23 (LOQ)	1.6	1.7 $\pm$ 0.2	0.053 $\pm$ 0.007 (LOD)	<1.20 (LOD)	0.031 $\pm$ 0.005 (LOQ)	<3.30 (LOQ)							
	Std. add.	2.7 $\pm$ 0.6		12.2 $\pm$ 2.6		17 $\pm$ 4		<0.23 (LOQ)		1.5 $\pm$ 0.4		<1.20 (LOD)		<3.30 (LOQ)								
SRM 3280 (multi-vitamin tablets)	Ext. calib.	1309 $\pm$ 215	10150 $\pm$ 810	0.08015 $\pm$ 1179	0.09067 $\pm$ 0.00086	0.2727 $\pm$ 0.02295	0.2963 $\pm$ 0.0024	—	—	—	—	17.67 $\pm$ 0.45	0.132 $\pm$ 0.45	<1.00 (LOD)								
	Std. add.	1374 $\pm$ 249		10140 $\pm$ 1300		0.08519 $\pm$ 0.01952		0.2894 $\pm$ 0.0679		—		17.58 $\pm$ 3.64		<1.00 (LOD)								
Pooled recovery (%)	Ext. calib.	99 $\pm$ 15	100 $\pm$ 14	103 $\pm$ 22	102 $\pm$ 16	103 $\pm$ 20	100 $\pm$ 20	6.8-13.2	105 $\pm$ 18	108 $\pm$ 17	106 $\pm$ 18	94 $\pm$ 17										
	Std. add.	102 $\pm$ 20		4.6-9.5		4.9-13.2		6.8-12.1		103 $\pm$ 22	103 $\pm$ 20	104 $\pm$ 21	105 $\pm$ 21									
Precision (%)	Ext. calib.	6.1-8.2	5.8-10.7	4.6-12.6	8.5-11.9	8.0-13.3	10.3-13.3	5.9-12.5	6.8-12.1	6.8-12.1	6.8-12.1	10.0-10.7	7.8-9.2									
	Std. add.	6.1-12.0	0.1-1.7	0.3-1.3	0.1-1.8	0.3-1.3	0.4-1.4	0.4-1.4	0.4-1.4	0.4-1.4	0.4-1.4	0.1-1.8	0.1-1.8	0.4-1.8								
z  score <sup>c</sup>	Ext. calib.																					

<sup>a</sup>  $U_{CRM}$  is the extended uncertainty from the certificate ( $k=2$ , 95% confidence level). <sup>b</sup>  $U_{lab}$  is the extended uncertainty in the laboratory ( $k=2$ , 95% confidence level). <sup>c</sup>  $|z|$  score calculated according to the Eurachem guide.<sup>40</sup>



**Table 3** Found concentrations in vegetables and meat-based CRMs obtained by the (HP-MAWD)-ICP-OES method for Cu, Zn, Cd and Pb using pneumatic nebulization and chemical vapor generation for Hg, Se and As

CRM	Cu		Zn		Cd		Pb		Hg		Se		As	
	Certified value $\pm$ $U_{CRM}^a$ (mg kg $^{-1}$ )	Found value $\pm$ $U_{lab}^b$ (mg kg $^{-1}$ )	Certified value $\pm$ $U_{CRM}^a$ (mg kg $^{-1}$ )	Found value $\pm$ $U_{lab}^b$ (mg kg $^{-1}$ )	Certified value $\pm$ $U_{CRM}^a$ (mg kg $^{-1}$ )	Found value $\pm$ $U_{lab}^b$ (mg kg $^{-1}$ )	Certified value $\pm$ $U_{CRM}^a$ (mg kg $^{-1}$ )	Found value $\pm$ $U_{lab}^b$ (mg kg $^{-1}$ )	Certified value $\pm$ $U_{CRM}^a$ (mg kg $^{-1}$ )	Found value $\pm$ $U_{lab}^b$ (mg kg $^{-1}$ )	Certified value $\pm$ $U_{CRM}^a$ (mg kg $^{-1}$ )	Found value $\pm$ $U_{lab}^b$ (mg kg $^{-1}$ )		
	Certified value $\pm$ $U_{CRM}^a$ (mg kg $^{-1}$ )	Found value $\pm$ $U_{lab}^b$ (mg kg $^{-1}$ )	Certified value $\pm$ $U_{CRM}^a$ (mg kg $^{-1}$ )	Found value $\pm$ $U_{lab}^b$ (mg kg $^{-1}$ )	Certified value $\pm$ $U_{CRM}^a$ (mg kg $^{-1}$ )	Found value $\pm$ $U_{lab}^b$ (mg kg $^{-1}$ )	Certified value $\pm$ $U_{CRM}^a$ (mg kg $^{-1}$ )	Found value $\pm$ $U_{lab}^b$ (mg kg $^{-1}$ )	Certified value $\pm$ $U_{CRM}^a$ (mg kg $^{-1}$ )	Found value $\pm$ $U_{lab}^b$ (mg kg $^{-1}$ )	Certified value $\pm$ $U_{CRM}^a$ (mg kg $^{-1}$ )	Found value $\pm$ $U_{lab}^b$ (mg kg $^{-1}$ )		
Tort-3 (lobster hepatopancreas)	497 $\pm$ 22	460 $\pm$ 61	136 $\pm$ 6	128 $\pm$ 23	42.3 $\pm$ 1.8	42.6 $\pm$ 4.9	0.225 $\pm$ <0.85	0.292 $\pm$ 0.018 (LOD)	10.9 $\pm$ 1.0 (LOD)	10.5 $\pm$ 1.6 (LOD)	59.5 $\pm$ 3.8 (LOD)	53.7 $\pm$ 7.8 (LOD)		
CE278k (mussel tissue)	5.98 $\pm$ 0.27	5.77 $\pm$ 1.36	71 $\pm$ 4	75 $\pm$ 11	0.336 $\pm$ 0.025	0.306 $\pm$ 0.084	2.18 $\pm$ 0.18 (LOQ)	<2.81 (LOQ)	<2.81 (LOQ)	<1.13 (LOQ)	1.62 $\pm$ 0.12 (LOQ)	1.80 $\pm$ 0.47 (LOQ)	6.7 $\pm$ 1.2 (LOQ)	
CS-M3 (dried mushroom powder)	18.73 $\pm$ 0.70	20.83 $\pm$ 3.28	113.30 $\pm$ 21.5	110.30 $\pm$ 0.110	1.229 $\pm$ 0.306	1.232 $\pm$ 0.108	1.863 $\pm$ 0.108 (LOQ)	<2.81 (LOQ)	2.849 $\pm$ 0.104 (LOQ)	2.662 $\pm$ 0.474 (LOQ)	17.43 $\pm$ 1.36 (LOQ)	16.91 $\pm$ 2.35 (LOQ)	0.651 $\pm$ 0.026 (LOQ)	
GBW 10011 (wheat)	2.7 $\pm$ 0.2	2.5 $\pm$ 0.4	11.6 $\pm$ 0.7	12.1 $\pm$ 1.8	18 $\pm$ 4	19 $\pm$ 5	0.065 $\pm$ 0.024 (LOD)	<0.85 (LOD)	1.6 (LOD)	1.7 $\pm$ 0.3 (LOD)	0.053 $\pm$ 0.007 (LOD)	<0.16 (LOD)	<0.06 (LOD)	
SRM 3280 multi-1400 $\pm$ 170	1470 $\pm$ 260	10 150 $\pm$ 810	9870 $\pm$ 1460	0.08015 $\pm$ 0.00086	<0.20 (LOQ)	0.2727 $\pm$ 0.0024 (LOD)	<0.85 (LOD)	—	—	17.42 $\pm$ 0.45 (LOQ)	11.73 $\pm$ 1.64 (LOQ)	0.132 $\pm$ 0.044 (LOQ)	<0.20 (LOQ)	
Pooled recovery (%)	100 $\pm$ 18	100 $\pm$ 16	—	99 $\pm$ 23	—	—	—	—	100 $\pm$ 17	—	102 $\pm$ 17	—	96 $\pm$ 16	
Precision (%)	6.6-11.8	7.3-9.7	—	—	5.8-13.7	—	7.3-8.9	—	4.6-13.1	—	7.2-9.2	—	—	
z  score <sup>c</sup>	0.3-1.8	0.3-1.0	—	—	0.1-0.8	—	0.2-0.8	—	0.4-0.8	—	0.3-1.8	—	—	

<sup>a</sup>  $U_{CRM}$  is the extended uncertainty from the certificate ( $k = 2$ , 95% confidence level). <sup>b</sup>  $U_{lab}$  is the extended uncertainty in the laboratory ( $k = 2$ , 95% confidence level,  $n = 3$  repeated measurements).

<sup>c</sup>  $|z|$  score calculated according to the Furachem guide.<sup>40</sup>

the standard addition method, compared to the certified values. The recoveries were within the range of 90–113%, with a trueness of 9–25% ( $k = 2$ ) for external calibration and 91–110% with a trueness of 9–27% for standard addition, respectively. This demonstrates that the (OFC)-SSETV- $\mu$ CCP-OES method is not affected by the non-spectral interferences from the sample matrix, and external calibration can be reliably used. According to the Eurachem Guide, the  $z$ -scores calculated for the found results using external calibration fell within the range of 0.1–1.8, lower than 2, which indicates a satisfactory performance without generating any signal of concern.<sup>40</sup>

In terms of As and Cd determination by SSETV- $\mu$ CCP-OES, it was previously shown that the determination of Cd at 228.802 nm cannot be performed in the presence of As, due to spectral interference from the As 228.812 nm line. This spectral line of As is approximately 25 times lower than that of Cd, and consequently, the LOD for As at 228.812 nm was  $2.8 \mu\text{g L}^{-1}$ , compared to  $0.12 \mu\text{g L}^{-1}$  for Cd when integrating the transient signal only at the CP. Under these conditions, a positive bias occurs in the determination of Cd at concentrations higher than  $8.5 \mu\text{g L}^{-1}$  As.<sup>31</sup> Considering the signal integration over 5 pixels on the spectral line profile, a LOD of  $2 \mu\text{g L}^{-1}$  As and a quantification limit of  $7 \mu\text{g L}^{-1}$  As are obtained, which could introduce a positive bias in the determination of Cd. This value is similar to the LOD of  $5 \mu\text{g L}^{-1}$  As at the 189.042 nm line. Therefore, in the present study, the determination of Cd at 228.802 nm and As was carried out using the following procedure. Two calibration curves were drawn for As at 189.042 nm and 228.812 nm using single-element solutions. A calibration curve was performed for Cd at 228.802 nm, using solutions in the absence of As. The As concentration in the sample was determined at 189.042 nm, and based on the calibration curve drawn at 228.812 nm, the emission signal was calculated when the As concentration exceeded  $5 \mu\text{g L}^{-1}$ . A signal correction of the sample was performed at 228.802 nm by subtracting the As signal from the total signal, thus obtaining the net signal of Cd in the sample. After correction, the concentration of Cd was determined based on the calibration curve drawn at Cd 228.802 nm.

Table 3 presents the results obtained for the determination of elements in the CRM samples using the ICP-OES method and HP-MAWD procedure and the generation of chemical vapor for Hg, As, and Se.

Data in Table 3 indicate recoveries ( $k = 2$ ) in the range of 91–111% by the (HP-MAWD)-ICP-OES method using pneumatic nebulization for Cu, Zn, Cd and Pb, and 90–111% for Hg, Se and As assisted by chemical vapor generation.

The Tukey statistical test showed that there is no significant difference ( $p < 0.05$ ) between the found values by the (OFC)-SSETV- $\mu$ CCP-OES method and those obtained by the reference ICP-OES method and sample preparation by HP-MAWD.<sup>41</sup>

### Applicability of the (OFC)-SSETV- $\mu$ CCP-OES method in real food samples

The results obtained for the determination of elements in fish tissue and mushrooms are presented in Table 4, while those for dietary supplements in Table 5. In the case of dietary supplements, the found concentration for the essential elements (Cu, Zn and Se) was compared to the targeted values declared on the label. The concentration of toxic elements (Cd, Pb, Hg, and As) was below the LOD of the method. The results indicated a precision of 4.9–14.5% for the (OFC)-SSETV- $\mu$ CCP-OES method, based on the combined uncertainty, which accounted for errors in the preparation of calibration standards and samples, calibration curve fitting, and aliquot analysis.

### Colours of the (OFC)-SSETV- $\mu$ CCP-OES method

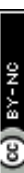
The whiteness of the (OFC)-SSETV- $\mu$ CCP-OES method was evaluated based on the comprehensive RGB 12 algorithm, which incorporates the redness, greenness, and blueness components.<sup>22</sup> The red component was assessed in accordance with the intended application and analytical performance, including LODs, precision, and accuracy. The AGREEprep metric was used for the evaluation of the green component, considering the reagent toxicity, amount of reagents, waste generated, energy consumption during sample preparation and analysis, and operator safety. The blue component considered cost- and time-efficiency, instrument miniaturization and operational simplicity, degree of automation, *on-line* applicability, portability, and potential for *on-site* measurements. The overall whiteness score was calculated as the average of the individual RGB scores. The greenness of the (OFC)-SSETV- $\mu$ CCP-OES method, compared to (OFC)-ICP-OES, (HP-MAWD)-SSETV- $\mu$ CCP-OES and (HP-MAWD)-ICP-OES, evaluated by the AGREEprep metric is presented in the SI (Fig. S6). Inputs used

**Table 4** Concentrations ( $\text{mg kg}^{-1}$ ) in real fish and mushroom samples obtained by (OFC)-SSETV- $\mu$ CCP-OES using external calibration

Sample	Mean concentration $\pm U_{\text{lab}}^a$ ( $\text{mg kg}^{-1}$ )							
	Cu	Zn	Cd	Pb	Hg	Se	As	
Fish tissue 1	$3.51 \pm 0.44$	$22.5 \pm 3.2$	<0.01 (LOD)	<0.07 (LOD)	<0.01 (LOD)	<1.20 (LOD)	<1.00 (LOD)	
Fish tissue 2	$0.835 \pm 0.125$	$8.00 \pm 1.30$	<0.01 (LOD)	<0.07 (LOD)	<0.01 (LOD)	<1.20 (LOD)	<1.00 (LOD)	
Mushroom 1	$54.0 \pm 11.5$	$118.4 \pm 17.8$	$0.318 \pm 0.044$	$0.423 \pm 0.071$	$0.062 \pm 0.018$	<3.96 (LOQ)	<1.00 (LOD)	
Mushroom 2	$42.4 \pm 7.5$	$129.8 \pm 15.8$	$0.124 \pm 0.019$	$0.794 \pm 0.125$	$0.671 \pm 0.157$	<3.96 (LOQ)	<1.00 (LOD)	
Mushroom 3	$71.8 \pm 7.0$	$116.0 \pm 15.2$	$0.263 \pm 0.057$	<0.231 (LOQ)	$0.506 \pm 0.073$	<3.96 (LOQ)	<1.00 (LOD)	
Mushroom 4	$41.3 \pm 9.2$	$85.8 \pm 12.4$	$0.192 \pm 0.024$	$0.345 \pm 0.082$	$0.209 \pm 0.042$	<3.96 (LOQ)	<1.00 (LOD)	
RSD (%)	4.9–11.1	6.1–8.1	6.3–10.8	7.9–11.9	7.2–14.5	—	—	

<sup>a</sup>  $U_{\text{lab}}$  is the extended uncertainty in the laboratory ( $k = 2$ , 95% confidence level,  $n = 3$  repeated measurements).



Table 5 Concentrations (mg per capsule) in real dietary supplements obtained by (OFC)-SSETV- $\mu$ CCP-OES using external calibration

Sample	Cu			Zn			Se		
	Declared value (mg per capsule)	Found value $\pm U_{lab}^a$ (mg per capsule)	Recovery $\pm U_{lab}^a$ (%)	Declared value (mg per capsule)	Found value $\pm U_{lab}^a$ (mg per capsule)	Recovery $\pm U_{lab}^a$ (%)	Declared value (mg per capsule)	Found value $\pm U_{lab}^a$ (mg per capsule)	Recovery $\pm U_{lab}^a$ (%)
Supplement 1	0.500	0.490 $\pm$ 0.062	98 $\pm$ 13	5	4.64 $\pm$ 0.61	93 $\pm$ 13	45	49.1 $\pm$ 6.0	109 $\pm$ 12
Supplement 2	2	2.16 $\pm$ 0.30	108 $\pm$ 14	25	26.7 $\pm$ 3.3	107 $\pm$ 12	—	—	—
Supplement 3	1.67	1.78 $\pm$ 0.28	107 $\pm$ 16	6.7	6.58 $\pm$ 0.69	98 $\pm$ 10	—	—	—
Pooled recovery $\pm U_{lab}^a$ (%)			104 $\pm$ 14		99 $\pm$ 12				109 $\pm$ 12
Precision (%)	0.4-1.2	6.3-7.9	0.4-1.2	5.2-6.6	5.2-6.6	0.4-1.2	5.2-6.6	5.2-6.6	6.1
z  score <sup>b</sup>									1.8

<sup>a</sup>  $U_{lab}$  is the extended uncertainty in the laboratory ( $k = 2$ , 95% confidence level,  $n = 3$  repeated measurements). <sup>b</sup> |z| score calculated according to the Eurachem guide.<sup>40</sup>

to assign AGREEprep scores for the evaluated methods are presented in the SI (Table S2). The colours corresponding to the (OFC)-SSETV- $\mu$ CCP-OES method, in comparison with (HP-MAWD)-GFAAS, (HP-MAWD)-ICP-OES and TDAAS methods for determination in foods, evaluated according to the RGB 12 algorithm, are presented in the SI (Fig. S7). Evaluation tables by the RGB 12 algorithm for these methods are presented in the SI (Table S3). The green score of the (OFC)-SSETV- $\mu$ CCP-OES method was evaluated at 77%, and attributed both to the virtually energy-free sample preparation by OFC (criterion 8), and the use of simple miniaturized instrumentation based on a very low energy and Ar consumption for microplasma generation and multielemental determination (criterion 9). Additionally, the OFC preparation method demonstrates a high degree of greenness due to the low sample consumption, minimal waste generation, and enhanced operator safety (criteria 4, 5 and 10). The green score decreases to 64% when analysis is performed using (OFC)-ICP-OES, due to the complexity of the instrumentation and the high energy and Ar consumption of the plasma source. The green score drops to 40% for (HP-MAWD)-SSETV- $\mu$ CCP-OES, even if the analysis is performed on a simple microplasma-based instrument. This decrease is attributed to the significantly higher consumption of  $\text{HNO}_3$ , larger sample and waste volumes generated, the high energy demand of HP-MAWD, and safety concerns arising from the potential risk of explosion of the digestion vessels (criteria 2, 4, 5, 8 and 10). The green score decreases to 26% when sample preparation and analysis involve the (HP-MAWD)-ICP-OES method and chemical vapor generation for Hg, As, and Se determination. The red score of the (OFC)-SSETV- $\mu$ CCP-OES method is 86%, slightly lower than the 94% of the GFAAS method, due to the poorer LODs associated with the microplasma source, despite its capability for simultaneous multielement determination. The SSETV- $\mu$ CCP-OES method offers a slightly higher red score due to its multielemental determination capability, compared to TDAAS (red score of 82%) exclusively designed for Hg determination.

The other performance parameters considered in the red score evaluation of the (OFC)-SSETV- $\mu$ CCP-OES method, namely precision and recovery, were considered comparable to traditional methods, such as ICP-OES and GFAAS. The highest blue score (98%), obtained for the (OFC)-SSETV- $\mu$ CCP-OES method, is attributed to the miniaturization and low-cost of the microplasma source and low-resolution microspectrometer, as well as the relatively high speed of sample preparation by OFC and simultaneous analysis (minimum 6 samples/hour). The green score of 94% for the microplasma-based analytical method coupled with OFC sample preparation is higher than that of GFAAS (81%) and ICP-OES with chemical vapor generation (69%) and is consistent with the results obtained through AGREEprep evaluation presented earlier. Although TDAAS is used only for Hg determination, it was evaluated to a green score of 98% in the RGB 12 algorithm owing to its ability to perform direct solid analysis without any reagent consumption. Overall, the whiteness score of the (OFC)-SSETV- $\mu$ CCP-OES method, evaluated by the RGB 12 algorithm, was 93%, compared to 86%, 82% and 76% for TDAAS, GFAAS and ICP-OES, respectively.

## Conclusions

It has been demonstrated that the coupling of fully miniaturized SSETV- $\mu$ CCP-OES instrumentation with sample dissolution assisted by OFC is a cost-effective approach and enables simultaneous multielemental determination in food, including priority hazardous elements (Cd, Pb and Hg). The method achieved the highest green score in the evaluation by the AGREEprep metric compared to ICP-OES coupled with the same sample preparation procedure, but especially when HP-MAWD was used. The RGB 12 algorithm also highlighted the attractiveness, effectiveness, and cost-efficiency of sample preparation by OFC with simultaneous analysis of microsamples using SSETV- $\mu$ CCP-OES. These critical analytical performances were highlighted by the high red and green scores, as well as the highest blue and white scores, in comparison with commercially available traditional spectrometric methods, such as GFAAS, TDAAS and ICP-OES. A substantial improvement in the SSETV- $\mu$ CCP-OES method sensitivity was obtained by integrating the analytical signal over the spectral line profile, generated by the CCD detector pixels of the microspectrometer, along with time-based integration of the episodic spectra signals, compared to transient signals integrated only on the central pixel of the analytical line. A significant improvement in LODs was obtained by integrating the signal over the spectral line profile on 5 pixels, this being a compromise between enhanced sensitivity and the increase in background signal noise, both associated with the number of pixels. The signal correction applied for Cd 228.802 nm, due to the spectral interference with the adjacent As 228.812 nm line, and using As determination at two wavelengths proved to be effective for Cd and As determination in food when a low-resolution microspectrometer is used. Supplementary studies are needed to improve the sensitivity for Se and As determination in foods by the (OFC)-SSETV- $\mu$ CCP-OES method through preconcentration after sample combustion. It is expected that the performance parameters of the method associated with the red, blue, green, and white scores to be enhanced, while the spectral interference between Cd and As at the most sensitive Cd 228.802 nm line to be avoided.

## Author contributions

Augustin Catalin Mot: writing – original draft; methodology, investigation, formal analysis, data curation, validation. Adrian-Ioan Dudu: methodology, investigation, formal analysis, data curation. Tiberiu Frentiu: supervision, project management, funding acquisition, writing – review & editing. Dorin Petreus: investigation, formal analysis. Erika-Andreea Levei: investigation, data curation. Zamfira Stupar: investigation, formal analysis. Maria Frentiu: investigation, formal analysis. Eniko Covaci: writing – review & editing, data curation, visualization, software, resources.

## Conflicts of interest

There are no conflicts to declare.

## Data availability

The data supporting this article have been included within the article and supplementary information (SI), while those mentioned by way of a simple summary statement are available from the corresponding author upon reasonable request.

Supplementary information is available. See DOI: <https://doi.org/10.1039/d5ja00297d>.

## Acknowledgements

This work was supported by a grant of the Romanian Ministry of Research, Innovation and Digitization, CNCS/CCCDI-UEFISCDI, contract no. 15PED/2025, project number PN-IV-P7-7.1-PED-2024-0091, within PNCDI IV. This work was also supported by a grant of the Romanian Ministry of Research Innovation and Digitization through the Core Program within the National Research Development and Innovation Plan 2022–2027, carried out with the support of MCID, project no. PN 23 05.

## References

- 1 E. H. Evans, J. Pisonero, C. M. M. Smith and R. N. Taylor, *J. Anal. At. Spectrom.*, 2025, **40**, 1136–1157.
- 2 M. Patriarca, N. Barlow, A. Cross, S. Hill, A. Robson and J. Tyson, *J. Anal. At. Spectrom.*, 2024, **39**, 624–698.
- 3 J. R. Bacon, O. T. Butler, W. R. L. Cairns, O. Cavoura, J. M. Cook, C. M. Davidson and R. Mertz-Kraus, *J. Anal. At. Spectrom.*, 2024, **39**, 11–65.
- 4 M. Ibourki, O. Hallouch, K. Devkota, D. Guillaume, A. Hirich and S. Gharby, *J. Food Compos. Anal.*, 2023, **120**, 105330.
- 5 J. Sneddon, C. Hardaway, K. K. Bobbadi and A. K. Reddy, *Appl. Spectrosc. Rev.*, 2006, **41**, 1–14.
- 6 E. M. M. Flores, J. S. Barin, M. F. Mesko and G. Knapp, *Spectrochim. Acta, Part B*, 2007, **62**, 1051–1064.
- 7 E. M. M. Flores and R. S. Picoloto, Sample Dissolution for Elemental Analysis/Oxygen Flask Combustion, 110–117, in *Encyclopedia of Analytical Science*, ed. P. Worsfold, C. Poole, A. Townsend and M. Miro, Academic Press, 3<sup>rd</sup> edn, 2019.
- 8 P. C. Crestani, T. C. Pereira, E. T. F. Larruscain, C. R. Laureano, E. M. M. Flores and F. A. Duarte, *Food Chem.*, 2023, **429**, 136916.
- 9 L. S. F. Pereira, G. D. Iop, M. S. Nascimento, L. O. Diehl, C. A. Buzzi, J. S. Barin and E. M. M. Flores, *J. Braz. Chem. Soc.*, 2016, **27**, 526–533.
- 10 J. S. F. Pereira, L. S. F. Pereira, L. Schmidt, C. M. Moreira, J. S. Barin and E. M. M. Flores, *Microchem. J.*, 2013, **109**, 29–35.
- 11 F. S. Rondan, G. S. Coelho Junior, R. M. Pereira, A. S. Henn, E. I. Muller and M. F. Mesko, *Food Chem.*, 2019, **285**, 334–339.
- 12 V. H. Cauduro, C. M. A. C. Alves, M. S. Nascimento, G. T. Druzian, F. P. Balbinot, M. F. Mesko and E. M. M. Flores, *Anal. Bioanal. Chem.*, 2024, **11**, 2859–2870.
- 13 G. Gohlke, T. C. Pereira, A. P. F. Padilha, C. R. Andriolli, A. S. Henn, R. S. Picoloto, P. A. Mello and E. M. M. Flores, *J. Food Compos. Anal.*, 2025, **144**, 107704.



14 J. P. Souza, C. Cerveira, T. M. Miceli, D. P. Moraes, M. F. Mesko and J. S. F. Pereira, *Food Chem.*, 2020, **321**, 126715.

15 G. S. Coelho Junior, V. P. Souza, J. Kratzer, J. Dedina and E. M. M. Flores, *Spectrochim. Acta, Part B*, 2024, **221**, 107055.

16 J. P. Souza, K. Kellermann, M. S. Camargo, D. P. Moraes, D. Pozebon and J. S. F. Pereira, *J. Anal. At. Spectrom.*, 2018, **33**, 1284–1291.

17 J. P. Souza, J. L. Boff, L. F. Rodrigues, D. P. Moraes and J. S. F. Pereira, *Anal. Methods*, 2022, **14**, 1285–1290.

18 W. Geng, T. Furuzono, T. Nakajima, H. Takanashi and A. Ohki, *J. Hazard. Mater.*, 2010, **176**, 356–360.

19 W. Geng, T. Nakajima, H. Takanashi and A. Ohki, *Fuel*, 2008, **87**, 559–564.

20 Y. Y. Ma, K. Zeng and T. C. Duan, *Microchem. J.*, 2019, **148**, 743–747.

21 W. Wojnowski, M. Tobiszewski, F. Pena-Pereira and E. Psillakis, *Trends Anal. Chem.*, 2022, **149**, 116553.

22 P. M. Nowak, R. Wietecha-Posluszny and J. Pawliszyn, *Trends Anal. Chem.*, 2021, **138**, 116223.

23 P. M. Nowak, *Green Chem.*, 2023, **25**, 4625–4640.

24 P. M. Nowak, W. Wojnowski, N. Manousi, V. Samanidou and J. Plotka-Wasylka, *Green Chem.*, 2025, **27**, 5546–5553.

25 P. M. Nowak, *Green Chem.*, 2025, **27**, 6699–6710.

26 N. Manousi, W. Wojnowski, J. Plotka-Wasylka and V. Samanidou, *Green Chem.*, 2023, **25**, 7598–7604.

27 P. M. Nowak and F. Arduini, *Green Anal. Chem.*, 2024, **10**, 100120.

28 C. M. Hussain, C. G. Hussain and R. Kecili, *Trends Anal. Chem.*, 2023, **159**, 116905.

29 F. A. Esteve-Turrillas, S. Garrigues and M. de la Guardia, *Trends Anal. Chem.*, 2024, **170**, 117464.

30 S. B. Angyus, M. Senila, T. Frentiu, M. Ponta, M. Frentiu and E. Covaci, *Talanta*, 2023, **259**, 124551.

31 S. B. Angyus, M. Senila, E. Covaci, M. Ponta, M. Frentiu and T. Frentiu, *J. Anal. At. Spectrom.*, 2024, **39**, 141–152.

32 B. D. Szeredai, T. Frentiu, N. Muntean, A. I. Dudu and E. Covaci, *J. Anal. At. Spectrom.*, 2025, **40**, 942–953.

33 P. W. J. M. Boumans, *Spectrochim. Acta, Part B*, 1991, **46**, 431–445.

34 P. W. J. M. Boumans, J. C. Ivaldi and W. Slavin, *Spectrochim. Acta, Part B*, 1991, **46**, 641–665.

35 T. Frentiu, M. Ponta, E. Darvasi, S. Butaci, S. I. Cadar, M. Senila, A. Mathe, M. Frentiu, D. M. Petreus, R. Etz, F. Puskas and D. Sulea, Miniaturized analyzer with Rhodium-filament evaporator for simultaneous determination of elements from liquid microsamples by optical emission spectrometry, *Romanian Pat.*, RO 131066 B1, State Office for Inventions and Trademarks, Bucharest, 2020.

36 D. Petreus, E. Plaian, A. Grama, E. Cordos and S. Cadar, Low power plasma generator at atmospheric pressure, *Romanian Pat.*, RO128077-B1, State Office for Inventions and Trademarks, Bucharest, 2016.

37 T. Frentiu, S. Butaci, E. Darvasi, M. Ponta, M. Frentiu and D. Petreus, *Chem. Pap.*, 2017, **71**, 91–102.

38 ISO 20236:2024, Water quality – Determination of total organic carbon (TOC), dissolved organic carbon (DOC), total bound nitrogen (TNb) and dissolved bound nitrogen (DNb) after high temperature catalytic oxidative combustion, International Organization for Standardization, Geneva, 2024.

39 J. Mandel, *The Statistical Analysis of Experimental Data*, Dover Publications, New York, 1964, pp. 272–309.

40 Eurachem Guide: Selection, Use and Interpretation of Proficiency Testing (PT) Schemes, ed. B. Brookman and I. Mann, 3<sup>rd</sup> edn, 2021, EPT\_2021\_P1\_EN.pdf, accessed 17 July 2025.

41 J. M. Tukey, *Biometrics*, 1949, **5**, 99–114.

42 A. I. Mihaltan, T. Frentiu, M. Ponta, D. Petreus, M. Frentiu, E. Darvasi and C. Marutoiu, *Talanta*, 2013, **109**, 84–90.

